Indian Journal of Radio & Space Physics
Vol. 22, February 1993, pp. 42-49

A comparison of aerosol size distributions obtained from bistatic lidar and low-pressure impactor experiments at a coastal station*

K Parameswaran & G Vijayakumar
Space Physics Laboratory, Vikram Sarabhai Space Centre, Thiruvananthapuram 695 022

Received 9 November 1992

Size distribution of aerosols in the atmospheric mixed region is studied using a bistatic CW lidar and a low-pressure impactor. Results obtained from these two experiments are compared. CW lidar observations showed that the size index (assuming the size distribution to follow a power law) generally lies in the range 3.5-5, whereas the size index obtained using the low-pressure impactor generally lies in the range 3.7-4.2.

1 Introduction

The characteristics of aerosols in the first few hundred metres above the ground largely depend on the local sources and sinks as well as on the prevailing meteorological conditions. Their characteristics vary from place to place depending on the topography and location (urban, rural, marine, etc.) of the observation site. These aerosols, which are significantly influenced by various natural processes and biological (including anthropogenic) activities, in turn, affect the terrestrial biological activity to a great extent. For example, during its atmospheric cycle, the sea salt aerosols in a marine environment play a pivotal role in the mechanism of precipitation, in the reduction of marine optical and infrared transmissivity, in the ocean to air transport of bacteria, etc. Hence a study of their physical and chemical characteristics is very important.

Different experimental methods are currently in use for the study of aerosols. But no single experiment can provide information on all the aerosol parameters. Remote sensing methods are very promising because of their operational conveniences as well as due to the fact that they do not directly affect the aerosol parameters being measured. They can also be used to study the aerosol characteristics at different altitudes as well as at remote places. However, the remote sensing methods depend upon certain reduction algorithms to deduce aerosol characteristics from measured quantities. On the other hand sampling methods have the advantage of direct measurement of the desired parameters. It is often necessary and useful to compare the characteristics of aerosols obtained by different methods to achieve consistent results.

Lidar is a valuable tool for sensing remotely the atmospheric aerosols. When operated in bistatic mode[1-3] it can provide information on scattering as a function of scattering angle, which is a very important input in the deduction[2,4] of aerosol characteristics. Size distribution of aerosols in the atmospheric boundary layer can be studied from the angular scatter measurements. In deducing the aerosol characteristics from these measurements, it is necessary to assume the basic form of the size distribution function. Usually a power law-type distribution is assumed for this purpose. Direct collection of particles by sampling can provide information on aerosol size distribution. The size and number distribution of atmospheric aerosols near the surface employing this technique has been the subject of a large number of investigations[5-8]. Various sampling methods[9] like impaction[10,11], filtration, and centrifugation are employed for this purpose. At Trivandrum (8.5°N, 77°E), a coastal station, we have carried out investigations on aerosol size distribution using bistatic lidar and direct particle sampling methods, and compared the results. In this paper, we present the results of this study.

2 Experimental set up and method of measurement

The bistatic CW lidar system consists of an ar-

*This paper was presented at the National Space Science Symposium held during 11-14 March 1992 at Physical Research Laboratory, Ahmedabad 380 009.

gon-ion laser transmitter and a transmission type (300 mm diam.) receiving telescope arranged in the same horizontal plane separated by a fixed distance of 380 m. The details of the lidar system and principle of operation are described elsewhere[12]. For conducting angular scatter observations, the transmitter and receiver are scanned in elevation at convenient steps such that the scattered radiation from a fixed altitude, 190 m, is received for different scattering angles[12]. Even though the range of possible scattering angles in this case is 90°-180°, angles above 165° are not used to avoid effects of any spatial inhomogeneities due to the large extent of the scattering volume. The angularly scattered intensity is measured for different scattering angles. Figure 1 shows the typical variation of the received signal with scattering angle for two days (23 Nov. 1989 and 23 Apr. 1992). The vertical lines parallel to Y-axis indicate the standard deviation of the signal representing the fluctuating component. The normalized signals corrected for the variation in scattering volume and path-lengths, which form the basic data for the present investigation, are obtained[4] from these angular scatter signals.

The aerosols close to the surface are directly sampled using a low-pressure impactor (LPI). The system (Andersen LPI Model 20-900) essentially consists of 14 collection stages[13] with 6 size ranges below 1.0 μm. Each stage contains a number of perforations with fixed diameters. The air containing aerosols is forced through these nozzles at a very high velocity and allowed to impinge on a flat surface (collection substrates) where some or all of the particles above a given mass (or diameter) are collected. The size of the nozzles determining the speed of the air at a flow rate decreases in subsequent stages from dimensions of several millimetres at the initial stages to tenths of millimetres at the final stage. Each collecting stage has a sigmoidal characteristics: small particles can pass with no deposition, a certain size range designated as cut-point for that stage is collected with 50% probability and significantly larger particles are collected completely. For a given pressure drop, the velocity through the nozzle will be fixed and hence the cut-point of that stage also will be fixed. Thus each stage of the impactor has a fixed cut-point for a given orifice pressure drop, which is different for different stages. These cut-points for different stages, shown in Table 1, range from 0.08 μm to 35 μm (aerodynamic diameters) if the system is operated at an orifice pressure drop of 114 Torr. When properly cascaded, each stage collects particles having aerodynamic diameters between its cut-point and that of the previous stage. These particles are collected on fibre glass substrates loaded in each of these stages. Mass of the particles collected in each size range is estimated by weighing the substrates before and after the collection using an electronic micro balance which can give the masses up to an accuracy of ± 5 μg. As the sys-

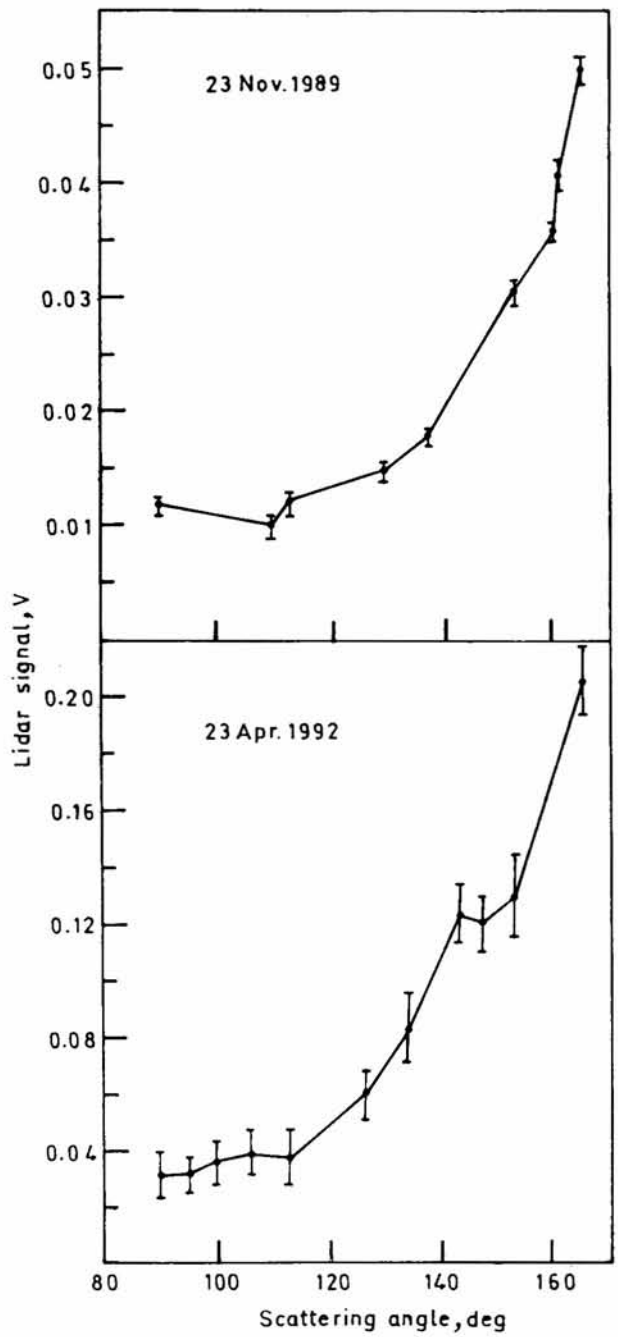

Fig. 1 – Variation of angularly scattered intensity from a fixed altitude (190 m) with scattering angle for 23 Nov. 1989 and 23 Apr. 1992.

Table 1 – Cut-points of different collection stages of the low-pressure impactor (LPI)

Stage	Cut-point aerodynamic diameter μm	Size range (aerodynamic diameters) of particles collected μm	Mean D_pP μm-ATM
0	35.0	>35	>35.1
1	21.7.	21.7-35	28.5
2	15.7	15.7-21.7	18.8
3	10.5	10.5-15.7	13.2
4	6.6	6.6-10.5	8.7
5	3.3	3.3-6.6	5.1
6	2.0	2.0-3.3	2.8
7	1.4	1.4-2.0	1.8
L_1	0.90	0.9-1.4	0.854
L_2	0.52	0.52-0.9	0.176
L_3	0.23	0.23-0.52	0.118
L_4	0.11	0.11-0.23	0.077
L_5	0.08	0.08-0.11	0.056
L_F	–	<0.08	<0.052

D_pP Product of aerodynamic diameter (D_p) and atmospheric pressure (P)

ATM Atmospheres

tem is operated at a constant orifice pressure, the velocity of the particles in each stage is known, using which the Stokes diameter can be estimated. From the mass of the aerosol particles collected in each size range thus obtained, the mass distribution, $dm(r)/dr$ (r being the particle radius), is obtained. The number-size distribution, $dn(r)/dr$, of aerosols is estimated from the mass distribution as[14,15]

$$\frac{dn(r)}{dr} = \frac{3}{4\pi r^3}\frac{dv(r)}{dr} = \frac{3}{4\pi r^3 \rho}\frac{dm(r)}{dr} \quad \ldots (1)$$

where ρ and $dv(r)/dr$ are respectively the mean density[16] and volume distribution of the aerosol particles.

The sampler (LPI) is operated few metres (~5 m) above the ground (so as to avoid surface effacts) for ~40 h. This sampling time is long enough to collect measurable samples and also small enough to avoid any saturation effect leading to particle bouncing. This sampling time is arrived at by trials satisfying these criteria. The collection substrates are properly pre-conditioned, and desiccated before and after the collection to eliminate the effect due to direct condensation of atmospheric water vapour.

3 Results

3.1 Aerosol size distribution from angular scatter observations

The method of obtaining aerosol size index from the angular scatter observations, presented in detail elsewhere by Parameswaran *et al.*[4,12], essentially assumes that the air molecules in the atmosphere are isotropic and do not scatter any intensity in the orthogonal direction, when the incident beam is linearly polarized with the electric vector orientation along the scattering plane (which is true for the lidar configuration used for the present study). In this case for a given scattering angle θ, the ratio of differential angular scattering cross-section of aerosols $\sigma_a(\theta)$, to the normalized signal $k(\theta)$, can be written as[4]

$$\frac{\sigma_a(\theta)}{k(\theta)} = \frac{\sigma_{a0}}{k_0} - \frac{n_m}{n_a}\frac{\sigma_m(\theta)}{k(\theta)} \quad \ldots (2)$$

where $\sigma_m(\theta)$ is the differential angular scattering cross-section of molecules for the scattering angle θ, σ_{a0} is the differential angular scattering cross-section of aerosols for $\theta = 90°$, k_0 is the normalized signal for $\theta = 90°$, and n_m/n_a is the ratio of the molecular number density to aerosol number density at the altitude (190 m in the present case) of scattering volume. The scattering angle θ is chosen such that the altitude of scattering volume is the same as that for $\theta = 90°$ (if there is any difference, this factor is to be accounted[4]). If $\sigma_a(\theta)/k(\theta)$ is plotted against $\sigma_m(\theta)/k(\theta)$ for different values of θ, the resulting curve will be close to a straight line if values of $\sigma_a(\theta)$ used are appropriate for the aerosols present in the scattering volume, and slope of this line will be n_m/n_a at 190 m. This property of Eq. (2) is used to evaluate the aerosol size index (ν) by making mass plots of the two ratios for different scattering angles and estimating the best-fit straight line. Different combinations of aerosol size distribution (power law indices) and refractive index (m) are used for this purpose. The differential angular scattering cross-section for each scattering angle evaluated for different combinations of aerosol size distributions (power law size index in the range 2-6) and refractive index (in the range 1.33-1.6) employing Mie theory is used to calculate the ratio $\sigma_a(\theta)/k(\theta)$. For each combination of ν and m, the cross correlation coefficient (R) is evaluated. When the assumed com-

bination (of aerosol parameters) is close to the real size distribution and refractive index of the aerosols present in the scattering volume, the correlation will be maximum (negative) and the intercept C will be close to the observed ratio of the differential angular scattering cross-section of aerosols to the normalized signal at $\theta = 90°$. To judge the fitness of the intercept a ratio Δ is defined such that

$$\Delta = (\sigma_{a0}/k_0 - C)/(\sigma_{a0}/k_0) \quad \ldots (3)$$

The combination of size distribution and refractive index for which the correlation coefficient (R) is highly negative and $|\Delta|$ is minimum is taken as the one consistent with our observations. Following this procedure, the values of (ν and m) for the observations on 23 Nov. 1989 and 23 Apr. 1992 are found to be (5 and 1.5) and (4.0 and 1.65) respectively. Using the above method, the aerosol size index is obtained on days on which angular scatter observations are conducted using the bistatic lidar for different days in the period 1985-92. These are presented in Table 2. The values of ν lie in the range 3.5-5. The most probable value of ν is found to be 4.5, which is the same as reported by Parameswaran *et al.*[4]

3.2 Size distribution from impactor experiment

Collection of particles using LPI is made on fibre glass substrates. The substrate which is to be loaded in each of the impactor stages is identified and kept in separate Petri dishes having identification marks. These substrates are pre-conditioned by first keeping them in a hot air oven (at 100°C) for about 1 h and then desiccating until they attain the room temperature. The initial mass of each substrate is then measured using a microbalance with an accuracy of ± 5 μg. These are then loaded at the respective stages of the impactor and taken to the sampling site (~ 5 m above the surface). The pump is switched on and the pressure at the critical orifice quickly adjusted to 114 Torr, which gives a flow rate of 3 litres of air per minute through different stages of the impactor. The sampling is continued for about 40 h and then terminated. The collection substrates are carefully removed from each stage of the impactor and are kept in the respective dishes. These collected substrates are desiccated for about 24 h before the final weighing. Substracting the initial mass of each substrate from the final mass, the mass of aerosol particles collected in each size range defined by the impactor cut-points are obtained. The particle size referred here is the aerodynamic diameter, which is defined as the diameter of a unit density sphere which would behave in the impactor in the same way as the particle (i.e., the diameter of a unit density sphere with the same terminal settling velocity as the particle).

Table 2 – Values of size index obtained from CW lidar experiment

Date	Size index (ν)
21 Mar. 1985	4.5
10 Apr. 1985	4.5
9 Aug. 1985	5.0
2 Sep. 1985	4.5
9 Sep. 1985	4.5
4 Oct. 1989	3.5
9 Nov. 1989	4.5-5.0
23 Nov. 1989	4.5-5.0
16 Jan. 1990	4.5
14 Feb. 1990	4.5
16 Aug. 1990	3.5-4.0
11 Oct. 1990	4.0
14 Nov. 1990	4.5
23 Apr. 1992	4.0

From the mass of aerosol particles collected in each stage, the cumulative percentage mass for aerosols smaller than a particular size (CPMS) is estimated. Typical plot of CPMS as a function of effective cut off aerodynamic diameter on a log-probability graph for two samples (April 1991 and March 1992) is shown in Fig. 2. The mass median diameter is the particle size for which the CPMS is 50%. This is ~ 3.4 μm for April 1991 and ~ 8 μm for March 1992. This shows that 50% of total mass collected is below 3.4 μm size in April 1991 whereas it is below 8 μm in March 1992. The CPMS curve is more or less linear for April 1991 but it shows small undulations for March 1992.

The Stokes diameter of a particle is defined as the diameter of the sphere with same density as the particle which would behave in the impactor in the same way as the particle (i.e., the diameter of a sphere of the same density as the particle with the same terminal settling velocity). From the aerodynamic diameters the Stokes diameter which is closer to the physical diameter of the particle can be calculated if the actual density of the aerosol particles is known. This also requires the aerosols to be homogeneous as to density. This is a

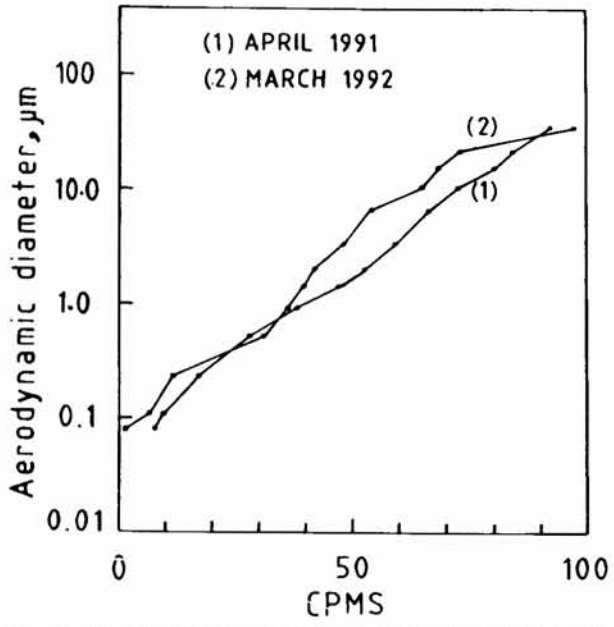

Fig. 2 – Cumulative size distribution curve for aerosols obtained using the low-pressure impactor during April 1991 and March 1992.

fairly valid assumption for natural atmospheric aerosols which can be taken to be a homogeneous mixture of particles produced from one or more sources. As the chemical composition of the aerosol particles is not known, using the available information on particle composition[17] near the surface at a coastal station like Trivandrum, the mean density of the particles can be approximated to 2.5 g cm^{-3} (Ref. 18). This value of ρ is used in our calculations.

The cut off value of D_pP (the product of aerodynamic diameter, D_p, and the atmospheric pressure, P, in which the LPI is operated incorporating the correction for slip factor) corresponding to one atmospheric pressure ($P \simeq 1$ atm.) is furnished by the manufacturers for each LPI stage, using which the mean value of D_pP (average of the cut off D_pP for a particular stage and that of its previous stage) is obtained. This mean value of D_pP for each stage, presented in the last column of Table 1, is divided by particle density (ρ) to obtain the equivalent aerodynamic term D_eP, and the Stokes diameter term (D_SP) is estimated using the impactor calibration chart (shown in Fig. 3) provided by manufacturers for the critical orifice pressure of 114 Torr. As the low pressure stages L_1 to L_5 are operated at 0.15 atm., D_SP of these stages obtained from the chart is divided by 0.15 to get the true Stokes diameters (D_S). But for the other stages (0 to 7) which are operated at $P = 1$ atm., the mean Stokes diameters are the same as

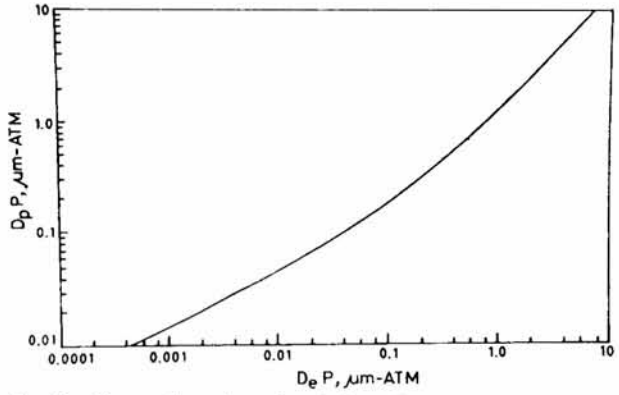

Fig. 3 – Conversion chart for Stokes diameter from aerodynamic diameter.

the D_SP values of the respective stages. Dividing D_S by 2, the Stokes radius, which is more closer to the geometrical radius of the particle (hereinafter will be referred to as the particle size), is estimated. Out of the 14 stages of the LPI excluding the first (0) and last (L_F) terminal stages, the remaining 12 size ranges (stages 1 to L_5), which are used in our present study, have mean Stokes radii (in μm) of 11.7, 7.7, 5.4, 3.5, 2.0, 1.0, 0.67, 0.31, 0.22, 0.11, 0.073 and 0.033 respectively. In the same way the Stokes radius ranges (dr and $d\log r$) for each size range, which are necessary for obtaining the mass-size distributions and number-size distributions, are also evaluated for each stage of LPI.

From the mass of aerosol particles collected in each stage, $dm(r)$, the mass distribution with particle size is obtained by plotting $dm(r)/d\log r$ verses r. Figure 4 shows the mass distribution with particle size during April 1991 and March 1992 for which the CPMS is shown in Fig. 2. The vertical lines parallel to Y-axis represent the error due to uncertainty in weighing the substrates (i.e., ± 5 μg in dm). As the LPI is operated at a constant flow rate of 3 litres/min for 40 h during each sampling cycle, the values of $dm(r)/d\log r$ for each stage is the mass of aerosol particles contained in the radius interval r and $r+dr$, contained in 7200 litres of air. The mass distribution per unit volume of air can then be obtained by dividing $dm(r)/dr$ with this volume of air. This is marked on the right hand side axis of Fig. 4.

The mass distribution shows a clear minimum around 2 μm in April 1991 whereas the minimum around 2 μm in March 1992 is rather broad. Except for two minor peaks (at $r = 0.1$ μm and $r = 3$ μm) the mass distribution remains almost constant with r in March 1992. The general form of the mass distribution curve for April 1991 is almost similar to that obtained by Khemani *et al.*[19]

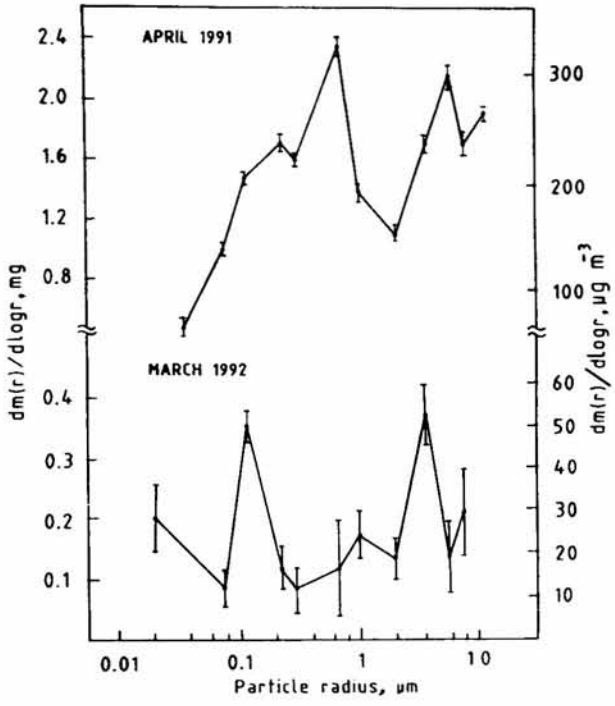

Fig. 4 – Typical mass distribution of aerosols obtained using the low-pressure impactor during April 1991 and March 1992.

for Poona, whereas that in March 1992 shows deviations. It may also be noted that the absolute value of $dm(r)/d\log r$ in April 1991 is 5 to 10 times more than that during March 1992.

From the values of $dm(r)$ for each LPI stage, $dm(r)/dr$ is estimated. From this the number-size distribution, $dn(r)/dr$, is obtained employing Eq. (1). Figure 5 shows these distributions for different months during the period 1990-92. Each curve in this figure represents the average size distribution of near surface aerosols spread over a period of 8 to 10 days in that month as the sampling time is spread over this period. In general, the number of particles decreases with increase in particle size, approximately following a power law. The size index corresponding to each of these distributions is estimated by least-square method considering all the points in the size range 0.03-11 μm which is almost the same as that assumed for obtaining size index from angular scatter observations of CW lidar[12]. The values of the size index for different months obtained using LPI are presented in Table 3. The size distribution curves also show small undulations (marked by vertical arrows in Fig. 5) indicating the presence of one or more modes in addition to the general power law behaviour. The values of r on which the mode appears in different months is also presented in Table 3. In all the months except

Table 3 – Aerosol size index, preferred modes and surface number density observed from the analysis of LPI data

Month	Size index	Modes μm	Surface aerosol number density $\times 10^4$ cm^{-3}
August 1990	4.05 ± 0.08	0.7	8.75
November 1990	4.22 ± 0.21	0.7	8.64
February 1991	3.86 ± 0.11	0.7	8.26
March 1991	3.97 ± 0.24	0.1,3.5	3.14
April 1991	3.97 ± 0.04	0.7	4.94
July 1991	3.83 ± 0.07	0.7	4.43
November 1991	3.80 ± 0.14	0.7,3.5	5.96
December 1991	3.80 ± 0.21	–	11.6
March 1992	3.91 ± 0.12	0.1,3.5	1.51

March 1991 and March 1992, this mode generally appears around 0.7 μm. In April 1991 and December 1991 the mode is rather weak. During March 1991 and March 1992 more than one mode appear—one close to 0.1 μm and the other close to 3.5 μm. By integrating the size distribution curve between the limits 0.03 μm and 11.7 μm, the total number of aerosol particles sampled is estimated. The number density of aerosols near the surface, obtained by dividing this total number of aerosols with the volume of air sampled in each sampling cycle, is also presented in Table 3. The near surface aerosol number density is maximum during winter months and minimum during March to July. Khemani *et al.*[19], from their impactor measurements at Poona, reported a similar feature—the total mass of particles collected being maximum in winter months.

4 Discussion

Tables 2 and 3 provide a direct comparison of the size index obtained using remote sensing (lidar) and direct sampling (LPI) methods. The values of the size index obtained by CW lidar experiment for different days during the period 1985 to 1992 lie generally in the range 3.5-5. These values are obtained from the angular scatter measurements conducted during a time interval of ~ 30 min at an altitude of ~ 190 m. Similarly the values of size index obtained from direct sampling techniques during the period 1990-92 lie in the range 3.7-4.2.

The CW lidar measures the size distribution of aerosols remotely at an altitude of ~ 190 m. The size distribution is obtained from the angularly scattered intensity, assuming horizontal stratification (within a few hundreds of metres) of spherical aerosol particles. The basic form of size dis-

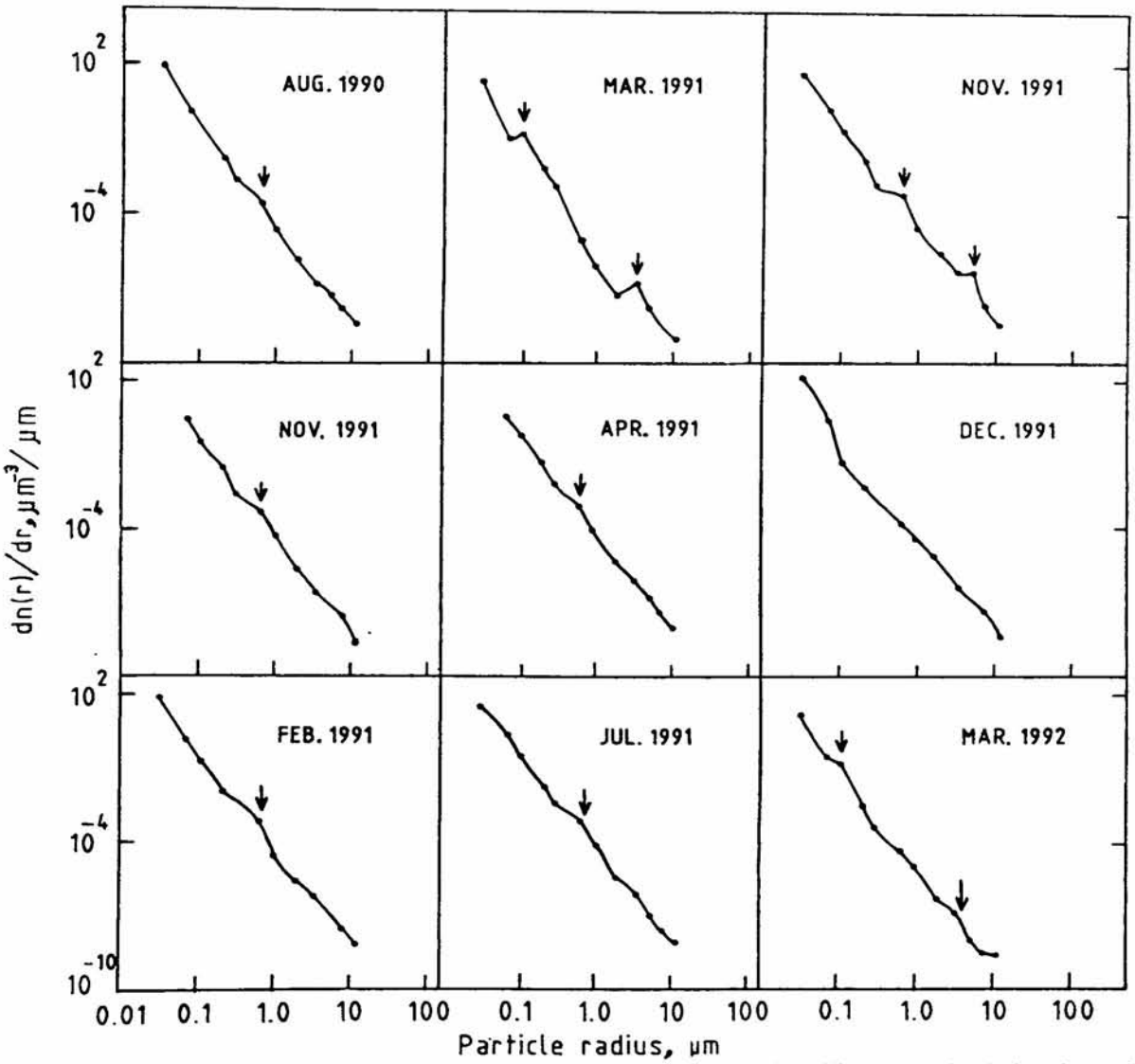

Fig. 5 – Size distribution of aerosols from the low-pressure impactor experiment for different months during the period August 1990-March 1992.

tribution is assumed to be of power law type. The size range of aerosols which contributes for scattering in the lidar wavelength is between 0.1 μm and 5μm. Even though the inversion assumes aerosol size distribution from 0.02 μm to 10 μm, aerosols in the size range 0.1-5 μm will be mainly affecting the estimated size distribution. As the complete measurement process takes only half an hour it can be considered to be almost an instantaneous measurement. The LPI measurements give the average size distribution close to the surface over a period of ~40 h spread over 8 to 10 days. Particles are assumed to be homogeneous having a constant density of ~2.5 g cm^{-3}. Thus, the involved assumptions and uncertainties in the two measurements are quite different. Within these limitations the general agreement between the size indices obtained from these two techniques is quite satisfactory. The assumption on the general form of the size distribution (power law) for CW lidar measurements seems to be quite reasonable as indicated by the LPI measurements.

The results obtained from these two experiments (though corresponding to different days) show that size distributions, in general, are quite similar at the two altitudes (5 m and 190 m). This means that in this altitude range the aerosols are well mixed and height of the mixing region in the early night hours (~1900 hrs) is more than 190 m. The altitude profiles of aerosols obtained from CW lidar experiment indeed show that the height of the mixing region is generally greater than 200 m (Ref. 12). The value of size index obtained in

the present investigation also matches well with the values reported by Pasceri and Friedlander[6], and Blifford and Ringer[8] for continental tropospheric aerosols at lower altitudes by direct sampling technique. Goel *et al.*[20] studied the size distribution of aerosols in the size range 0.2-5.0 μm using a four-stage impactor at Roorkee, and observed that the size index generally lies in the range 4-5. It may be noted that the present comparison can be considered to be direct only for August 1990 and November 1990 and may be for March-April 1992. For these months there is a satisfactory agreement between the size indices obtained from the two experiments. For the other months, LPI and lidar data do not correspond to the same month. So in these cases the general form of the size index obtained from these two experiments only can be compared. The values of ν obtained from LPI seems to be, in general, slightly on the lower side as compared to those obtained using CW lidar. This is quite reasonable as the number of large particles will be more near the surface compared to at 190 m, resulting in a decrease of the size index.

Even though the general form of size distribution in Fig. 5 can be best approximated to a power law, as noted earlier, it shows small undulations. Thus these distributions can also be represented as a combination of one or more log-normal distributions or a combination of power law with log-normal distributions. In such cases, the mode radius of these log-normal distributions will appear as cusps in the resulting distribution. The undulations in Fig. 4 can be attributed to this. The value of r for which the mode appears in each month is tabulated in Table 3. From this it is seen that the mode around 0.7 μm appears to be present during all the months except during March. This matches very well with the large particle mode seen in the solar radiometer measurements[21] at Trivandrum. The small particle mode observed in solar radiometer derived size distributions (~ 0.3 μm) is not seen in the LPI derived size distributions. This indicates that particles causing the mode at 0.7 μm in solar radiometer measurements are mainly confined to the atmospheric mixed region whereas the small particle mode would have been caused by particles in the free troposphere above. During the month of March the mode around 0.7 μm becomes weak whereas a small particle mode at ~ 0.1 μm and a large particle mode around 3.5 μm appear. This feature is observed in March 1991 as well as in March 1992. The mode during March 1992 is rather weak. Thus, the size distribution near the surface shows variation with season. A larger data base is required to quantify these seasonal variations. However, these finer details of size distribution (presence of modes) cannot be delineated from bistatic lidar observations.

Acknowledgements

The authors thank Dr B V Krishna Murthy for his valuable suggestions during the preparation of this manuscript and Dr K Krishna Moorthy and Mr P Pradeepkumar for their excellent co-operation in conducting the CW lidar experiment. They are also thankful to the Analytical and Spectroscopy Division of VSSC for its valuable support in preconditioning and weighing the substrates.

References

1 Regan J A & Herman B M, *Proceedings of the 14th Radar Meteorology Conference* (American Meteorological Society, Boston, Massachusetts, USA), 1970, 275.
2 Ward G, Cushing K M, McPeters R D & Green A E S, *Appl Opt (USA)*, 21 (1973) 2585.
3 Devara P C S & Ernest Raj P, *J Aerosol Sci (GB)*, 20 (1989) 37.
4 Parameswaran K, Rose K O & Krishna Murthy B V, *J Geophys Res (USA)*, 89 (1984) 2541.
5 Junge C E, *J Meteorol (USA)*, 12 (1955) 13.
6 Pasceri R E & Friedlander S K, *J Atmos Sci (USA)*, 22 (1965) 579.
7 Clark W E & Whitby K T, *J Atmos Sci (USA)*, 24 (1967) 677.
8 Blifford I H & Ringer L D, *J Atmos Sci (USA)*, 26 (1969) 716.
9 Pueschel R F, *Probing the atmospheric boundary layer* (American Meteorological Society, Boston, Massachusetts, USA), 1987.
10 May K R, *J Sci Instrum (USA)*, 22 (1945) 147.
11 Anderson A A, *Am Ind Hyg Ass J (USA)*, 27 (1966) 160.
12 Parameswaran K, Jain Thomas, Rose K O, Satyanarayana M, Selvanayagam D R & Krishna Murthy B V, *Study of aerosols in the lower troposphere using a bistatic CW lidar*, Sci Rep SPL:SR:003:87 (Space Physics Laboratory, Vikram Sarabhai Space Centre, Trivandrum, India), 1987.
13 McFarland A R, Nye H S, Erickson C H, *Development of low-pressure impactor*, EPA Rep # 650/2-74-014 (US Environmental Protection Agency, Research Triangle Park, North California, USA), 1973.
14 Hidy G M, *Aerosol—an industrial & environmental science* (Academic Press Inc, New York), 1963.
15 Junge C E, *Air Chemistry and Radioativity* (Academic Press Inc, New York), 1963.
16 Goroch A K, Fairall C W & Davidson K L, *J Appl Meteorol (USA)*, 21 (1982) 666.
17 Zhou M Y, Yang S J, Parungo F P & Harris J M, *J Geophys Res (USA)*, 95 (1990) 1779.
18 Pruppacher H R & Klett J D, *Microphysics of clouds and precipitation* (D Reidal Publishing Co., USA), 1978.
19 Khemani L T, Momin G A, Naik M S, Vijayakumar R & Ramana Murty Bh V, *Tellus (Sweden)*, 34 (1982) 151.
20 Goel R K, Varshneya N C & Verma T S, *Ann Geophys (France)*, 3 (1985) 339.
21 Krishna Moorthy K, Prabha B Nair & Krishna Murthy B V, *J Appl Meteorol (USA)*, 30 (1991) 844.